Mechanism of Edge Localized Mode mitigation by Resonant Magnetic Perturbations

M.Bécoulet[1], F.Orain[1], G.T.A.Huijsmans[2], S.Pamela[3], P. Cahyna[4], M.Hoelzl[5], X. Garbet[1], E. Franck[5], E. Sonnendrücker[5], G. Dif-Pradalier[1], C.Passeron[1], G. Latu[1], J. Morales[1], E. Nardon[1], A. Fil[1], B. Nkonga[6], A. Ratnani[6], V. Grandgirard[1]

[1]CEA, IRFM, 13108 Saint-Paul-Lez-Durance, France
[2]ITER Organization, Route de Vinon-sur-Verdon, 13067 St Paul Lez Durance, France
[3]CCFE, Culham Science Centre, Oxon, OX14 3DB, UK
[4]Institute of Plasma Physics ASCR, Prague, Czech Republic
[5]Max-Planck-Institut, Garching, Germany
[6] Nice University, INRIA, Sophia Antipolis, Equipe CASTOR, France

A possible mechanism of Edge Localized Modes (ELMs) mitigation by Resonant Magnetic Perturbations (RMPs) is proposed based on the results of non-linear resistive MHD modelling using the JOREK code, Realistic JET-like plasma parameters and RMP spectrum of JET error-field correction coils (EFCC) with main toroidal number $n=2$ were used in the simulations. Without RMPs, a large ELM relaxation is obtained mainly due to the most unstable medium-n ballooning mode. The externally imposed RMP drives non-linearly the modes coupled to $n=2$ RMP which produce small multi-mode relaxations, mitigated ELMs. The modes driven by RMPs exhibit a tearing-like structure and produce additional islands. Mitigated ELMs deposit energy into the divertor mainly in the structures ("footprints") created by $n=2$ RMPs, however, slightly modulated by other non-linearly driven even harmonics. The divertor power flux during ELMy phase mitigated by RMPs is reduced almost by a factor of ten. The mechanism of ELM mitigation by RMPs proposed here reproduces generic features of high collisionality RMP experiments, where large ELMs are replaced by small much more frequent ELMs or magnetic turbulence. Total ELMs suppression was also demonstrated in modelling at higher RMP amplitude.

1.Introduction. The aim of the ITER project is the demonstration of the scientific feasibility of nuclear fusion reactor based on a magnetic confinement concept as a future source of energy [1]. Plasma edge magneto-hydro-dynamic (MHD) instabilities, such as ELMs driven by the pressure gradient and the plasma current produce quasi-periodic relaxations of the edge density and temperature profiles on few hundred microseconds time scale. ELMs in ITER are predicted to lead to the transient heat fluxes reaching tens of GWm^{-2} which would cause strong erosion of the PFC materials [1-2], hence ELMs control is mandatory in ITER. Recently the application of Resonant Magnetic Perturbations (RMPs) demonstrated the possibility of total ELMs suppression or strong mitigation of their size [3-9], motivating the use of this method in ITER [1]. In the last decade, the non-linear MHD theory and modeling have made a significant progress to refine the understanding of ELM [10-14] and RMP [15-20] physics. However the understanding of RMP interaction with ELMs is still missing and was not modeled so far, motivating work we are presenting here. One can clearly distinguish two groups of RMP experiments. At high collisionality the application of RMPs usually leads to the replacement of large ELMs by small frequent ELMs or MHD turbulence, the divertor power loads are reduced by RMPs. Small changes in edge pressure gradient and MHD stability are reported [3-8]. On the other hand, at low collisionality resulting from strong density pump-out due to RMPs, ELMs have been totally suppressed in DIII-D and the plasma edge appears to be stable to peeling/ballooning modes [9].

In the present Letter we report on the first observation of ELM mitigation by RMPs in non-linear resistive MHD simulations done with the code JOREK in toroidal geometry including confined plasma region, X-point, Scrape Off Layer (SOL) and divertor [14]. The results we found in modelling correspond to generic features observed in high collisionality RMP experiments. The JOREK model used here includes two-fluid diamagnetic effects important in the pedestal region and is described in details in [18]. The realistic JET pulse #77329 parameters used as in [17,18,19]: $R_0=2.9m$, $a=0.89m$, $B_{tor}=1.8T$, $q_{95}=3.8$. The density and

temperature profiles were approximated with the following central and pedestal values: $T_e(0)=6keV$, $T_{e,ped}=1.8keV$, $T_i=T_e$, $n_e(0)=5.10^{19}m^{-3}$, $n_{e,ped}=3.310^{19}m^{-3}$. The toroidal rotation profile was taken parabolic with a central frequency $\Omega_\phi(0)=38krad/s$. Resistivity and viscosity are temperature dependent, the central value of Lundquist number was taken $S\sim10^7$, which for numerical reasons is lower compared to the experimental value ($S=10^9$). In the typical JOREK run initially the equilibrium with flows is obtained for the toroidal harmonic $n=0$ (axisymmetric component) on a time scale of $\sim 1ms$ [18]. After that, for ELMs modelling, other harmonics are initialized in plasma at "noise" level ($\sim10^{-25}$). In the case of RMPs vacuum amplitude for corresponding harmonic (here $n=2$ from EFCC [6,17,19]) is set at the boundary and increased in time until the stationary conditions are reached [18], resulting in a 3D equilibrium, then other harmonics were initialized to study interaction of ELMs with RMPs.

2. Main results. In Fig.1 the time evolution of the magnetic energy is presented for two cases. The first one corresponds to the non-linear modelling of an unmitigated ELM where the harmonics $n=0$ and $n=2,4,6,8$ were taken into account . As appeared after numerical tests (not presented) n>8 modes growth rates were smaller due to the diamagnetic stabilization [14] so they were excluded from modelling to save computational time. The axisymmetric component $n=0$ is coupled non-linearly to all harmonics permitting self-consistent modelling of the profile evolution due to ELMs and RMPs. Note that on the linear stage the most unstable mode is $n=8$, the $n=2$ mode is stable. Approaching the ELM crash (maximum of magnetic energy for $n=8$) all modes grow due to the non-linear coupling [11, 21] but $n=8$ remains the largest one. After the crash, the magnetic energy starts to decrease since the transport generated during the ELM [10,11] leads to a relaxation of the edge pressure profile, removing the drive for the ELM instability. Note also that for a linear run (without mode coupling) the single mode $n=2$ remains stable (Fig.1). In the second case, $n=2$ RMPs were applied at the computational boundary and progressively increased until the magnetic energy of RMP reaches a stationary value. After that, the other modes $n=4,6,8$ are included into the simulation. In this case the behavior of all modes is quite different: the magnetic energies of the $n=4:8$ oscillate in time with similar maximal amplitudes, much smaller than $n=8$ in unmitigated ELM. The power and heat fluxes on the divertor plates are reduced about by a factor of ten with RMPs (Fig.2), corresponding to experiment [5]. The magnetic energy of the modes in the mitigated ELMs decreases while of EFCC current increases as illustrated on Fig.3. The test run with $n=1,2,...8$ with $\Delta n=1$ without and with RMP confirmed that mitigated ELMs consist of even modes coupled with $n=2$ RMP and the odd modes ($n=1,3,5,7$) remain on the noise level in spite of the fact that linear growth rates of $n=8$ and $n=7$ modes were very similar in ELM without RMPs (not presented). The initial energies for even harmonics increase with the EFCC current, due to the stronger coupling with $n=2$ RMP (Fig.4), the reason why they are dominant with RMPs compared to odd harmonics, but the question is why ballooning modes ($n=7,5$) which were unstable without RMPs are not developing? The first hypothesis we tested was that the enhancement of the edge transport by RMPs reduces pressure gradient and hence growth rates of the modes and consequently the ELM size. Yet, a simulation without RMPs at artificially lowered pressure gradient (down to a level corresponding to the pressure gradient with RMPs -*"low P"* on Fig.5-6 demonstrates only a slight reduction of the $n=4:8$ mode growth rates in the linear stage (Fig.6), but the $n=8$ mode remains the most unstable and produces a large ELM (not presented here). The detailed analysis of the time evolution of the growth rates of the mode $n=8$ in the early (linear) stage is presented in Fig.6 for different cases. The time traces for each case were shifted in time correspondingly in order to compare the growth rates before the first relaxation in each run. During the exponential growth of the mode, the growth rate is almost constant which is the case for the unmitigated ELM, at lower pressure gradient *("lowP")* without RMPs and at low

RMP amplitude (*4kAt*). At larger RMPs (>20kAt), the strictly speaking "linear" stage of the *n=8* mode does not exist anymore. The growth rates oscillate in time, leading on average to an even slower growth of the mode. In the case when 3D magnetic topology with RMP at *40kAt* is established and then *n=4-8* modes are initialized, the *n=8* mode grows similarly as in an unmitigated ELM if the non-linear coupling for n=8 mode is switched off in the code (case "*40kAt,lin*"on Fig.6). Summarizing, this analysis suggests that neither only the reduced pressure gradient nor only the modified 3D magnetic topology induced by RMPs lead to ELM mitigation without non-linear coupling: both only slightly reduces the linear growth rate of the mode *n=8*, but the large ELM due to *n=8* mode still happens with a certain time delay. Only the case with the non-linear coupling of the modes demonstrated the ELM mitigation. The emerging physical picture we propose here is the following. In a natural ELM, the most unstable mode (here *n=8*) should reach a sufficiently large level of perturbations to create conductive heat transport along perturbed magnetic field lines and convective **ExB** density transport for the profiles relaxation in ELM [10,11]. If externally applied RMP (here *n=2*) amplitude is not strong enough in plasma, the transport due to RMPs only reduces the growth rates of the modes, but it is not sufficient for the pedestal to become completely stable for ballooning/peeling modes, mitigated ELMy regime occur. The modes mostly strongly coupled to RMP are growing from already initially large amplitude and quickly reach a sufficient level to produce additional to RMP transport to the SOL. Hence RMP is a constant strong non-linear drive for these modes. The magnetic energy now is distributed between the modes *n=2,4…8*, increasing energy in *n=2,4,6* harmonics and decreasing energy of the *n=8* mode compared to the natural ELM case. Thus the ELM energy "cascades" non-linearly towards lower *n*-numbers [22], observed in KSTAR RMP experiments [23]. As a result the relaxations due to the multi-modes can manifest themselves as more frequent small ELMs or MHD turbulence similar to Type II ELMs providing sufficient transport and hence preventing large ELM crash due to a single most unstable mode which has no time to grow. It's important to note that with RMPs the "ballooning" nature of the modes changes to tearing-like parity ($\psi_{n,m}\neq 0$ on the corresponding rational *q=m/n* surface as compared to the ballooning–like parity ($\psi_{n,m}= 0$ on *q=m/n*) [22]) , since they are driven by RMPs. It is clearly seen from the comparison of the edge magnetic topology (Fig.7). For the case of the natural ELM one observes typical ballooning distortion of the magnetic surfaces due to mode *n=8* (Fig.7(a)). The corresponding "footprints" in the outer divertor show a clear *n=8* structure (Fig.8(a)). The magnetic topology with *n=2* RMPs (Fig.7(b)) indicates that only the very edge is ergodic: this is due to the rather strong screening of RMPs rotation in the pedestal region [18]. The corresponding footprints (Fig.8(b)) show a typical static *n=2* structure. In the ELMy regime mitigated by RMP with *n=2* the very edge keeps mainly an *n=2* structure, but new island (*m/n=9/4, 14/6* and *15/6*) occur on the corresponding rational surfaces (Fig.7(c)). The corresponding footprints keep the *n=2* structure imposed by external RMPs, being modulated by the presence of *n=4,6,8* modes(Fig.8(c)). Note that similar footprints of ELMs with RMPs were reported in experiments [24]. This paper is essentially devoted to the description of the mitigated by RMPs ELMy regimes. Note however that the total ELM suppression can be obtained if RMP amplitude in plasma is large enough to produce sufficient transport reducing the pedestal pressure gradient to the values when peeling-ballooning modes are totally stabilized leading to total ELM suppression regime [3]. The case of total ELM suppression is presented in Fig.9 for slightly different plasma parameters, where diamagnetic term was artificially increased by ~10% and natural ELM was due to the most unstable mode *n=6*. Characteristic ELM cycles due to *n=6* mode relaxation observed without RMPs disappear with RMP *n=2* at *80kAt* (Fig.9).

Conclusions. ELM mitigation by RMPs was demonstrated in the non-linear resistive MHD modelling using the JOREK code [10,18]. Realistic JET plasma parameters and the RMP

spectrum of EFCC ($n=2$) were used. In unmitigated ELM, medium $n=8$ was the most unstable mode, producing a large ELM crash. The mitigated ELMs consist of the modes non-linearly driven by RMPs, which have a tearing-like structure, generating islands and additional to RMP edge ergodisation leading to the continued transport from the pedestal to SOL. Mitigated ELMs represent more frequent small relaxations compared to a large "natural" ELM crash. The divertor power flux is reduced almost by a factor of ten by RMPs. Divertor footprints of mitigated ELMs exhibit mainly structures created by $n=2$ RMPs, modulated by other low n modes. The mechanism of ELM mitigation by RMPs proposed and modelled here reproduces many generic features of high collisionality ELM mitigation regimes observed in experiment, where large ELMs are replaced by small frequent ELMs or broad band magnetic turbulence [3-5,9,24]. Total ELMs suppression was also demonstrated in modelling at higher RMP amplitude.
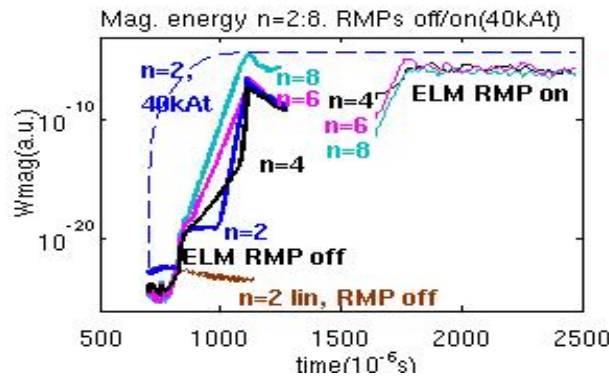
Acknowledgments.

Fig.1. Magnetic energy ($\sim|\psi_n|^2$) of modes $n=2:8$ in natural and mitigated ELMs with $n=2$ RMP at 40kAt.

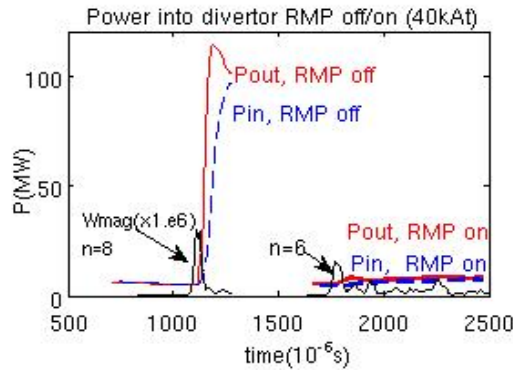*Fig.2. Power to inner and outer divertor in natural and mitigated by RMPs ($n=2$, 40kAt) ELMs.*
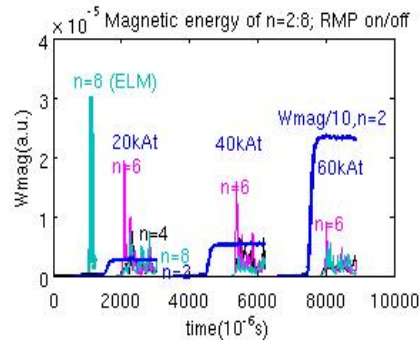
Fig.3. Magnetic energy of modes n=2:8 in natural and mitigated ELMs at EFCC current scan.
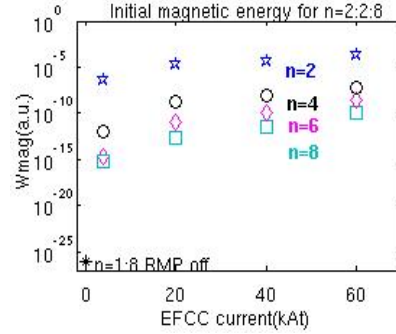

Fig.4. Initial magnetic energy of even harmonics coupled to n=2 RMP.
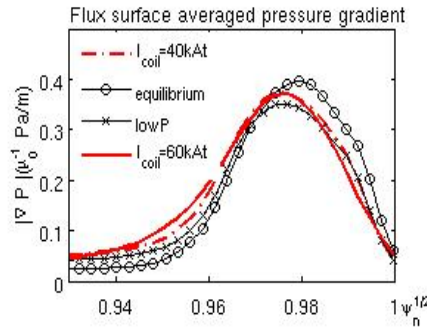

Fig.5. Flux averaged edge pressure gradient before an ELM w/o RMP, at lower initial pressure w/o RMP, and at 40 and 60 kAt EFCC current.
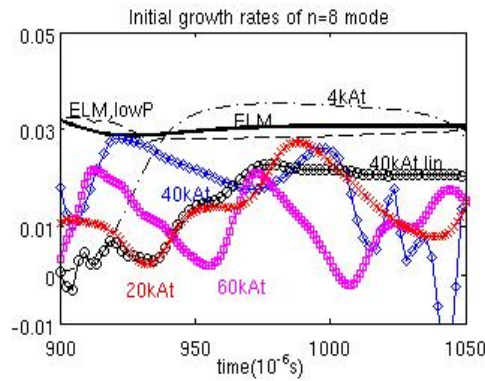

Fig.6. The initial growth rate of n=8 mode in natural ELM (bold); at lower pressure gradient (dashed); with RMP at 4kAt (dot-dashed); at 20kAt (cross); at 40 kAt (diamonds) ; at 40kAt in linear run for n=8 (3D equilibrium)- in circles; at 60kAt (squares).
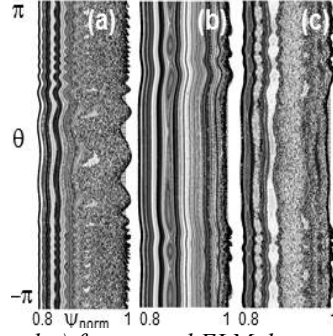
Fig.7. Edge magnetic topology (Poincare plot) for natural ELM due to n=8 mode (a), with RMP n=2,40kAt-(b), with mitigated by RMPs ELMs(c). Coordinates are geometrical poloidal angle and normalized poloidal flux.
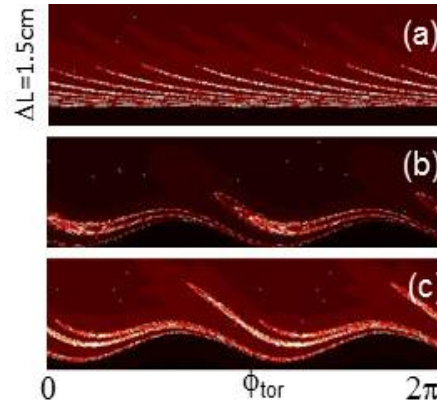

Fig.8. Footprints in the outer divertor in the natural n=8 ELM -(a), with RMP n=2(40kAt)-(b), with mitigated ELMs(c). Brighter colors indicate longer connection length.
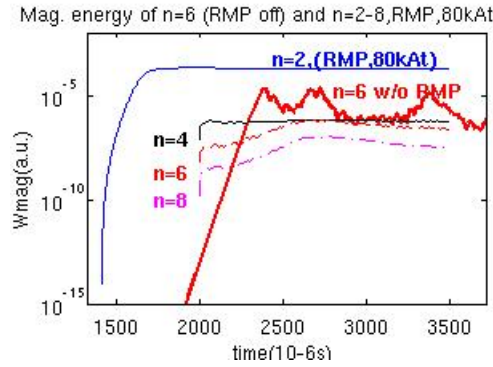

Fig.9. Magnetic energy in ELMs due to n=6 mode without RMP (in bold) and magnetic energy in n=2:8 modes in total ELM suppression regime with RMP n=2 at 80kAt.

References:

[1] R Hawryluk et al. Nucl. Fus 49(2009) 065012
[2] A Loarte A. et al Plasma Phys. Control. Fusion 45(2003)1549
[3] Evans T.E. et al Phys. Rev. Lett 92(2004) 235003
[4] W. Suttrop et al Phys Rev Lett 106(2011)225004
[5] Y M Jeon et al Phys. Rev. Lett. 109(2012)035004
[6] Y Liang et al Phys Rev Letters 98(2007)265004
[7] J M Canik et al Nucl Fusion 50(2010)034012
[8] A Kirk et al Phys. Rev. Lett. 108(2012)255003
[9] M Fenstermacher et al Phys of Plas15(2008)56122
[10] G T A Huysmans et al Plasma Phys Control Fusion 51 (2009) 124012
[11] G T A Huijsmans and A. Loarte, Nucl. Fusion 53 (2013) 123023
[12] S Pamela et al Plasma Phys. Control. Fusion 55 (2013) 095001

[13] L E Sugiyama et al Phys of Plasmas 17(2010)062505
[14] Xu X.Q. et al Phys. Rev. Lett 112 (2014) 085001
[15] H Strauss et al Nucl Fusion 49 (2009) 055025
[16] N Ferraro et al Nucl Fusion 53 (2013) 073042
[17] M Becoulet et al Nucl Fusion 52 (2012)
[18] F Orain et al Phys of Plasmas 20(2013)102510
[19] M Becoulet Nucl Fusion 48 (2008) 024003
[20] F LWaelbroeck et al Nucl Fusion 52 (2012) 074004
[21] I Krebs et al Phys of Plasmas 20(2013)082506
[22] D Biskamp "Non-linear magnetohydrodynamics" Ch.7, Cambridge Monographs on Plasma Phys 1, 2004.
[23] G S Yun et al Phys Rev Lett 107(2011) 045004
[24] M.W Jakubowski Nucl Fusion 49 (2009) 095013